Chapter 4

RAPID STELLAR ROTATION: CENTRIFUGAL EFFECTS

And the light shone in darkness and
Against the Word the unstilled world still whirled
About the centre of the silent Word.

T. S. Eliot, *Ash Wednesday*

In this Chapter we begin to study the impact of rotation on a star and its wind. Dynamics in a noninertial reference frame requires the consideration of fictitious forces, such as the centrifugal and Coriolis forces for uniform rotation, in order to be able to express, e.g., Newton's laws of classical motion in the standard manner. However, we wish to solve for the stellar wind in the *inertial* (nonrotating) frame, and the centrifugal and Coriolis forces become embedded in the non-Cartesian spherical geometry terms ($\propto v^2/r$) in the momentum conservation equations, eq. (2.5)–(2.7). Before dealing with the effect of these terms on an expanding wind, though, we must assess how the underlying stellar interior and photosphere are affected by rotation (Section 4.1). Only then can we begin to examine the interaction between the now-moving atmosphere and the radiation-driven wind. Expansion in the equatorial plane ($\theta = \pi/2$) is studied in Section 4.2, where we find that steady-state wind solutions may not exist for sufficiently rapid rotation. Finally, the form of the Sobolev line force is re-examined in Section 4.3, and we discuss the possible existence of "shear" wind solutions which can drastically alter the angular momentum of the wind.

4.1 Oblateness and Gravity Darkening

Tassoul (1978) and Smith (1987) review the physics of rotating stellar interiors, and conclude that most normal main sequence and giant stars rotate nearly uniformly. Although evolution may lead to significant differential rotation in the deep interior, observational constraints are still quite ambiguous, and most observations are consistent with uniform or near-uniform rotation. The most obvious effect of rotation on the star is that it becomes flattened, or *oblate*. As opposed to incompressible fluid bodies, centrally-condensed stars do not conserve volume upon increasing their rotation velocity; Papaloizou & Whelan (1973) found the maximum decrease in the polar radius to be only $\sim 3\%$, but the maximum increase in the equatorial radius to be as much as $\sim 50\%$. Let us then assume that a star's polar radius R_p is a constant, and determine how its shape at other latitudes depends on rotation.

The gravitational potential of a uniformly rotating body can be approximated by assuming a pointlike concentration of mass M_* at its center, and superposing a standard "centrifugal" term,

$$\Phi(r,\theta) = -\frac{GM_*}{r} - \tfrac{1}{2}\Omega^2 r^2 \sin^2\theta \quad . \tag{4.1}$$

These are the so-called *Roche equipotentials* (named for the French mathematician Edouard Albert Roche), where Ω is the constant angular velocity of the body. The surface of a rotating star will be confined to equipotential surfaces, and if the polar ($\theta = 0$) radius $r = R_p$ is specified, the potential at the pole can be compared to that at an arbitrary polar angle θ,

$$-\frac{GM_*}{R_p} = -\frac{GM_*}{R_*} - \tfrac{1}{2}\Omega^2 R_*^2 \sin^2\theta \quad , \tag{4.2}$$

and we obtain the shape of the axisymmetric (ϕ-independent) stellar surface $r = R_*(\theta)$ by solving the above cubic equation for R_*. Note that the use of a more self-consistent, e.g., polytropic, mass distribution yields less than a 1% change in the oblate surface radius derived with the Roche model (see Orlov 1961).

In practice, the angular velocity Ω is not always initially known – the actual velocity at the star's equator $V_{\rm eq}$ may be specified in its place. There are thus at least two possible ways to solve for $R_*(\theta)$:

1. **Ω known:** First note that a "critical" or "breakup" angular velocity $\Omega_{\rm crit}$ can be defined, for which $\nabla\Phi$ has zero magnitude at the equator ($\theta = \pi/2$). When $\Omega = \Omega_{\rm crit}$, the radius $R_*(\pi/2) \equiv R_{eq}$ reaches its maximum possible value of

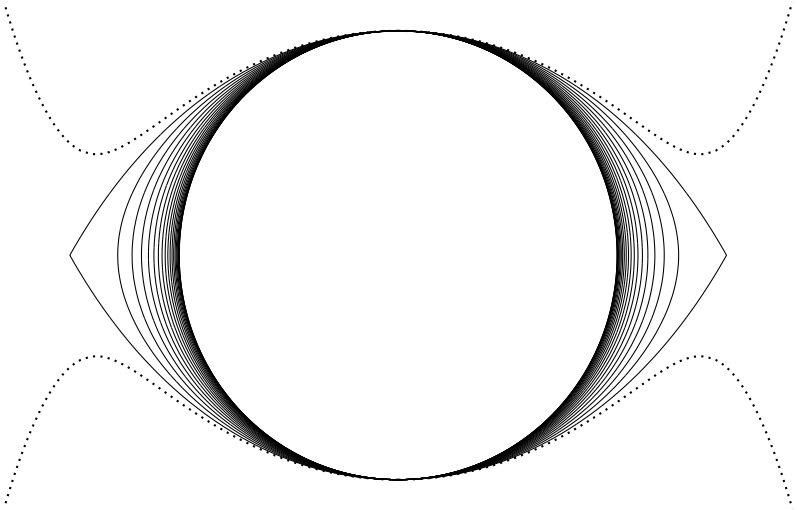

Figure 4.1: Equatorial cross sections of Roche equipotential surfaces, plotted for a uniform distribution of ω values between 0 and 1.05, at increments of 0.05. The dotted curve is a representative post-breakup surface ($\omega = 1.05$).

$R_{eq} = (3/2)R_p$. When $\Omega < \Omega_{\rm crit}$, one can define the fractional angular velocity ω as $\Omega/\Omega_{\rm crit}$, and

$$\Omega = \omega\Omega_{\rm crit} = \omega\sqrt{\frac{GM_*}{R_{eq}^3}} = \omega\sqrt{\frac{8GM_*}{27R_p^3}} \ , \tag{4.3}$$

where $0 \leq \omega \leq 1$ for a closed stellar equipotential. The cubic potential equation (eq. [4.2]) can thus be expressed as

$$\frac{4}{27}\omega^2 x^3 \sin^2\theta - x + 1 = 0 \ , \tag{4.4}$$

where $x = x(\omega,\theta) \equiv R_*(\theta)/R_p$, and solved via trigonometric methods (see Collins 1963; Collins & Harrington 1966) by

$$x(\omega,\theta) = \frac{3}{\omega\sin\theta}\cos\left[\frac{\pi + \cos^{-1}(\omega\sin\theta)}{3}\right] \ . \tag{4.5}$$

Figure 4.1 shows cross sections of these Roche surfaces for a uniformly spaced distribution of ω values between 0 and 1.05, at intervals of 0.05. Note the "cusp" at the equator of a critically-rotating star, where gravity exactly balances the centrifugal force, and the outward equatorial flaring of a model star rotating faster than its breakup velocity.

2. $\boldsymbol{V_{\rm eq}}$ **known:** Since $V_{\rm eq} = \Omega R_{eq}$, the above cubic potential equation can be rewritten as

$$w_o\left(\frac{R_*}{R_{eq}}\right)^2 \sin^2\theta - 1 + \frac{R_p}{R_*} = 0 \ , \tag{4.6}$$

defining $w_o \equiv V_{\rm eq}^2 R_p/2GM_*$. At the equator ($R_* = R_{eq}, \theta = \pi/2$), this equation becomes

$$w_o - 1 + \frac{R_p}{R_{eq}} = 0 \ , \tag{4.7}$$

and $(R_p/R_{eq}) = (1 - w_o)$. The variable w_o ranges from zero ($V_{\rm eq} = 0$) to $\frac{1}{3}$ ($V_{\rm eq} = \Omega_{\rm crit}R_{eq}$), and the general cubic equation becomes

$$w_o(1 - w_o)^2 x^3 \sin^2\theta - x + 1 = 0 \ , \tag{4.8}$$

and, by comparing with eq. (4.4) above, we find that

$$\omega^2 = \frac{27}{4}w_o(1 - w_o)^2 \ , \tag{4.9}$$

and we can use the same trigonometric solution (4.5) to determine the radius $x = R_*/R_p$. Many authors express a star's rotation in terms of a *fractional equatorial velocity,* i.e., $(V_{\rm eq}/V_{\rm crit})$, and this ratio is given by

$$\Upsilon \equiv \frac{V_{\rm eq}}{V_{\rm crit}} = \omega \frac{R_{eq}}{R_{eq,{\rm crit}}} = 2\cos\left(\frac{\pi + \cos^{-1}\omega}{3}\right) \quad . \tag{4.10}$$

Both ω and Υ vary monotonically from 0 to 1, but "median" values of Υ correspond to more "extreme" values of ω (e.g., when $\Upsilon = 0.5$, $\omega = 0.6875$). Thus, despite the more fundamental nature of ω, the fractional velocity Υ more evenly spans the range of oblateness from $x_{eq} = 1$ to 1.5.

Note that the Roche gravitational potential, as defined above, does not include any terms due to radiation pressure or force. As a useful first approximation to the inclusion of such terms, the mass of the star M_* can be replaced by an effective mass term, $M_*(1-,\ )$, where $,$ is the electron scattering Eddington factor introduced in Section 2.2.2. This term is negligible in all but the Wolf-Rayet, O, and earliest B type stars. For the standard ζ Puppis model star of Chapter 2, the Eddington ratio $, = 0.351$, which results in a critical rotation velocity of $V_{\rm crit} = 510.4\,{\rm km\ s^{-1}}$. This is significantly higher than the observed $V_{\rm eq}\sin i$ of 210–230 km s^{-1}, for which the Roche oblateness is only a $\sim$ 6–7% effect at the equator.

In the star's atmosphere one can define radial and latitudinal components of the effective gravity by examining the gradient of the potential Φ:

$$g_r = -\frac{\partial\Phi}{\partial r} = -\frac{GM_*}{r^2} + \Omega^2 r\sin^2\theta = \frac{GM_*}{R_p^2}\left(-\frac{1}{x^2} + \frac{8}{27}x\omega^2\sin^2\theta\right) \quad , \tag{4.11}$$

$$g_\theta = -\frac{1}{r}\frac{\partial\Phi}{\partial\theta} = \Omega^2 r\sin\theta\cos\theta = \frac{GM_*}{R_p^2}\left(\frac{8}{27}x\omega^2\sin\theta\cos\theta\right) \quad . \tag{4.12}$$

Thus, $|\mathbf{g}|^2 = g^2 = g_r^2 + g_\theta^2$, because the azimuthal component of the effective gravity (g_ϕ) is identically zero from meridional symmetry. Note, of course, that this effective gravity applies only on the oblate stellar surface, and not in the wind (which does *not* rotate rigidly). At the equator ($\theta = \pi/2$), the radius at which the effective gravity vanishes is given by $x_{g=0} = 1.5\,\omega^{-2/3}$, and for $\omega = 1$ this occurs precisely at the "cusp" on the surface of the critically-rotating star.

The early work of von Zeipel (1924) and Chandrasekhar (1933) showed that a distorted gaseous star in hydrostatic equilibrium exhibits a change in its net radiative flux which is proportional to the local gravity over its surface. This "gravity darkening" can be qualitatively understood by assuming the condition of *hydrostatic*

equilibrium in the interior of a star, in which the effective gravity $\mathbf{g}$ is derivable from a scalar potential Φ,

$$\nabla P = \rho \mathbf{g} = -\rho \nabla \Phi \quad . \tag{4.13}$$

Because the normals to the surfaces of constant Φ and constant P are anti-parallel, the gas pressure P must be constant on equipotential (constant Φ) surfaces. Thus P must be a function of Φ only, and the density ρ can be expressed as

$$\rho = \frac{|\nabla P(\Phi)|}{|\nabla \Phi|} = -\frac{dP}{d\Phi} \quad , \tag{4.14}$$

assuming the density is monotonically stratified. Thus, in these cases, ρ must be a function of Φ as well. Also, if the atomic abundances (i.e., μ in eqs. [2.11] and [2.12]) are considered constant along equipotentials, the temperature T must also be a function of Φ only. In *radiative equilibrium*, the flux carried outward by photons is given by the conductive term,

$$\boldsymbol{\mathcal{F}} = -\frac{16\,\sigma_B}{3\,\bar{\kappa}\,\rho}\,T^3\,\nabla T \quad , \tag{4.15}$$

where σ_B is the Stefan-Boltzmann constant and $\bar{\kappa}$ is the Rosseland mean absorption coefficient (in cm^2/g), and is a function of the state variables ρ, P, and T. Thus, one can write

$$\nabla T = \frac{dT}{d\Phi}\,\nabla \Phi \tag{4.16}$$

using the chain rule of differentiation, so that the flux can be concisely expressed as

$$\boldsymbol{\mathcal{F}} \;=\; f(\Phi)\nabla\Phi \;=\; -f(\Phi)\,\mathbf{g} \quad , \tag{4.17}$$

where $f(\Phi)$ is constant along an equipotential surface. This expression violates *strict* radiative equilibrium, in which $\nabla \cdot \boldsymbol{\mathcal{F}} = 0$, and thus some non-rotational fluid flow must arise to compensate for the resulting local heating and cooling of gas. However, the time scale of such "meridional circulation" flow (Eddington 1929; Sweet 1950) is usually much too long to significantly affect the validity of the gravity darkening flux derived above.

Slettebak (1949) discussed the variation in effective temperature $T_{\rm eff}$ over the surface of rotationally distorted single stars. Since the total luminosity L_* of the star is equivalent to the flux integrated over its surface, its magnitude is

$$\mathcal{F} = \sigma_B T_{\rm eff}^4(\theta) = K_{vz}\,g(\theta) \quad , \tag{4.18}$$

with von Zeipel's constant K_{vz} given by the constraint that the total integrated flux gives L_*, no matter the degree of rotation, and

$$K_{vz} = \frac{L_*}{\oint g\,dS} \quad , \tag{4.19}$$

where the integral in the denominator is taken over the entire surface of the star. We implicitly assume that the bolometric luminosity L_* remains constant for a given model star rotating at different rates, but this is not strictly true. Because the presence of centrifugal forces weakens the effective gravity in the interior, the central conditions mimic those of a nonrotating star of lower mass. Thus the central temperature and luminosity are lower in rotating stars, but the maximum effects for uniform rotation are quite small; L_* decreases by only 5–10% at the critical rotation velocity (Papaloizou & Whelan 1973).

The evaluation of von Zeipel's constant, though straightforward, involves a complicated integral. The magnitude of the effective gravity g depends on the above solution for the latitudinally-dependent Roche radius $R_*(\theta)$, and the element of surface area is

$$dS = \frac{[R_*(\theta)]^2}{\cos\delta} \sin\theta \, d\theta \, d\phi \quad , \tag{4.20}$$

where δ is the angle between the local gravity and the radius vector ($\cos\delta = -g_r/g$), and takes into account the fore-shortening of the surface area. Note that, in the fully radiative case, the effective temperature is dependent on the gravity raised to the power 0.25. For stars in which convection plays a non-negligible role, however, the variation of flux with gravity is not so simply parameterized. If the exponent (sometimes termed b), which is 0.25 in the radiative case, can take on other values, the gravity darkening is described as

$$\sigma_B T_{\rm eff}^4 = \left(\frac{L_*}{\Sigma_{4b}}\right) g^{4b} \quad , \tag{4.21}$$

where the function Σ_{4b} is given by

$$\Sigma_{4b} \equiv \oint g^{4b} dS = 2\pi \int_0^\pi \frac{g^{4b} R_*^2 \sin\theta \, d\theta}{\cos\delta} \quad , \tag{4.22}$$

and the two limiting cases of $b = 0$ and 0.25 give the surface area of the star (Σ_0) and the surface-weighted gravity (Σ_1), respectively. The values of Σ_0 and Σ_1 have been computed via numerical quadrature, and can be fit via least squares as power series in the fractional angular velocity ω,

$$\begin{aligned} \Sigma_0 &\approx 4\pi R_p^2 \left[1 + 0.19444\,\omega^2 + 0.28053\,\omega^4 - \right. \\ &\quad \left. 1.9014\,\omega^6 + 6.8298\,\omega^8 - 9.5002\,\omega^{10} + 4.6631\,\omega^{12}\right] \qquad (4.23) \\ \Sigma_1 &\approx 4\pi G M_* \left[1 - 0.19696\,\omega^2 - 0.094292\,\omega^4 + \right. \\ &\quad \left. 0.33812\,\omega^6 - 1.3066\,\omega^8 + 1.8286\,\omega^{10} - 0.92714\,\omega^{12}\right] \quad . \qquad (4.24) \end{aligned}$$

Using only even powers of ω gives a much-improved fit over using the same number of free parameters for even and odd powers together. The relative error in these fits

is rather small, but it is slightly dependent on ω. For $\omega < 0.9$, the error is $< 1\%$ for Σ_0 and $< 0.2\%$ for Σ_1. For all ω $(0 < \omega < 1)$, the error is $< 2\%$ for Σ_0 and $< 0.6\%$ for Σ_1.

Lucy (1967) derives $b \simeq 0.08$ for late-type main-sequence stars. Using classical mixing-length computations (Baker & Temesváry 1966), Lucy utilizes the condition that the gradient of the specific entropy vanishes in a fully convective zone to set the limits of state variable structure integrations over the stellar surface. This method is questioned by Anderson & Shu (1977), who find that if flux is carried exclusively by standard mixing-length convection from the deeper layers upward, the photosphere should eventually radiate it away at a constant rate $\sigma_B T_{\rm eff}^4$, independent of the gravitational potential Φ. This implies $b = 0$, and predicts an isothermal effective temperature distribution for main sequence stars later than spectral type $\sim$ F7, but the exponent b can supposedly range from 0 to 0.25 for spectral types $\sim$ F2 to F7. Earlier type stars, however, exhibit the standard radiative $b = 0.25$.

Osaki (1970) treats the problem more generally. The exponent b, in a situation where the radiative and convective contributions to the net flux vary with depth, can be determined numerically, at least to first order, as an eigenvalue of the energy transfer equation in the convective envelope. Zhou & Leung (1990) emphasize the fact that, for systems obeying both hydrostatic and thermal equilibrium, surfaces of constant temperature and pressure do not necessarily coincide. Thermal stability will thus cause convective circumfluence between different latitudes, and Coriolis forces thus play a non-negligible role in the outer layers of such rotating stars. Clearly the present theoretical understanding of *convective* gravity darkening is far from complete, but the von Zeipel result for early-type stars with mainly *radiative* envelopes is definitely on firmer ground.

4.2 Centrifugal Wind Modulation

The wind from a rapidly rotating star will have different properties at different latitudes, and under certain circumstances may vary in all three dimensions and in time. For the present, however, we confine our models to the *equatorial plane,* where rotation has the strongest impact, and where the flow can be constrained to a surface of constant colatitude, $\theta = \pi/2$. (See Pizzo 1982 for discussion of similar approximations in modeling the solar wind.) Thus the θ (latitudinal) component of the momentum conservation equation is assumed satisfied in the equatorial plane by the trivial solution $v_\theta(\theta = \pi/2) = 0$, i.e., no latitudinal flow into or out of the computational domain, with all partial derivatives in the θ direction considered negligible. In this Section we examine two effects which can modulate and redistribute the mass flux from a rotating star: the centrifugal decrease in the effective gravity

(which also causes oblateness) and flux redistribution due to gravity darkening.

4.2.1 Mass Loss Enhancement due to Centrifugal Forces

Following Gerasimovič's (1934) suggestion that the rapid rotation of a star makes it easier for material to be accelerated from the surface, many models of "centrifugally enhanced" winds from hot stars have been constructed (Limber 1964; Friend & Abbott 1986; Pauldrach, Puls, & Kudritzki 1986; Poe 1987; Bjorkman & Cassinelli 1993). Let us review these models and explore the dynamical consequences of this enhanced mass loss on Sobolev mCAK winds. The ϕ (azimuthal) component of the momentum conservation equation is given, in the equatorial plane, by

$$\frac{\partial v_\phi}{\partial t} + v_r \frac{\partial v_\phi}{\partial r} + \frac{v_\phi}{r \sin\theta} \frac{\partial v_\phi}{\partial \phi} = -\frac{v_r v_\phi}{r} - \frac{1}{\rho r \sin\theta} \frac{\partial P}{\partial \phi} \quad , \tag{4.25}$$

but if we assume a time-steady and *azimuthally symmetric* wind (i.e., with vector components such as $v_\phi \neq 0$, but all $\partial/\partial\phi = 0$) only the two terms proportional to v_r survive, and

$$v_r \left(\frac{\partial v_\phi}{\partial r} + \frac{v_\phi}{r} \right) = 0 \quad . \tag{4.26}$$

In the deep photosphere, where $v_r \to 0$, this equation does not necessarily constrain v_ϕ, so we assume $v_\phi(r = R_*) = V_{\rm eq}$ as a lower boundary condition. In the wind, where $v_r \neq 0$, the above equation demands that v_ϕ conserve angular momentum, and that

$$v_\phi(r) = \frac{V_{\rm eq} R_*}{r} = \frac{\Omega R_*^2}{r} \quad . \tag{4.27}$$

To generalize to stellar latitudes other than the equator ($\theta = \pi/2$), one can replace $\Omega \to \Omega \sin\theta$, but keep in mind that two- or three-dimensional effects will dominate the flow at latitudes other than $\theta = 0$ or $\pi/2$, and the inclusion of this one-dimensional centrifugal term then becomes highly suspect (see Chapter 5).

The angular-momentum-conserving rotation of the stellar wind affects the radial momentum equation (eq. [2.5]) by the term proportional to v_ϕ^2/r, and this can be treated as a contribution to the effective gravity,

$$g_{\rm eff} = -\frac{GM_*(1 - ,)}{r^2} + \frac{\Omega^2 R_*^4}{r^3} \quad . \tag{4.28}$$

This rotation term drops off more rapidly in radius than gravity, so that even if it has a strong impact near the star, it can be neglected as $r \to \infty$. Because rotation *reduces* the effective gravity near the surface, it has the ability to induce a greater mass flux. This can be estimated using the methods of Section 2.3.2, where we

assumed a zero sound speed and a critical radius (for finite disk models) extremely close to the surface ($r_c \approx R_*$). Thus, the CAK equation of motion becomes

$$F_1 \approx w + (1-, -\Theta) - \frac{C}{1+\alpha} w^{\alpha} = 0 \ , \tag{4.29}$$

where $\Theta \equiv \Omega^2 R_*^3 / GM_* = 8x^3\omega^2(1-,)/27$, and the effective gravity term $(1-, -\Theta)$ consistently replaces $(1-,)$ in the critical point conditions (eq. [2.107]) and the CAK mass loss rate (eq. [2.110]). This approximation for the increase in the mass loss rate compares well with the results of more complex numerical calculations. Note, however, that the local mass flux of the equatorial wind, defined by the equation of continuity (eq. [2.9]), is not equivalent to the *total* mass loss rate of the star, but is expressed as a spherically integrated flux ($4\pi r^2 \rho v$) for convenience.

As the denser wind from a rotating star accelerates outward, the $1/r^3$ term in the effective gravity eventually dies away, and it reverts to its nonrotating value. Because the mCAK radiative force is proportional to the inverse of the density, the acceleration on this higher-$\dot{M}$ material is smaller, and the terminal velocity v_∞ *decreases* for the more rapidly rotating winds. This can be seen heuristically from the infinite-radius v_∞ equations in Section 2.3.2, and especially from the approximate solution, eq. (2.123). Note that here the quantity $(1-,)$ is not modified by Θ, because we are at an infinite radius, but C is lower because of the increased mass loss rate. Poe (1987) and Koninx (1992) noted that for a sufficiently high rotation velocity the wind becomes so dense that the line force cannot drive it to infinity, and this corresponds to the imaginary solutions of eq. (2.123) for too-small values of C.

Figure 4.2 shows the velocity laws $v_r(r)$ for numerical mCAK models of the standard ζ Puppis star of Chapter 2, rotating in the equatorial plane at various rotation speeds. For these models, the equatorial radius is kept fixed at R_p, and the effects of gravity darkening on the mass loss rate are ignored. Both the decrease in v_∞ (as originally modeled by Friend & Abbott 1986) and the termination of the steady-state wind at a finite radius r_t (the "Koninx effect") are evident. Koninx (1992) showed that a new singular locus appears at large radii for rotating wind solutions, and the accelerating mCAK velocity laws intersect it non-tangentially. Thus, without the opportunity to *graze* this singular locus, as occurs near the star, the time-steady wind solutions become non-analytic for $r > r_t(V_{\rm eq})$. Note also that as $V_{\rm eq}$ increases, r_t decreases, and the critical radius r_c increases. For a large enough rotation speed, then, the two singular loci merge together, and do not even allow a partially analytic wind.

For the ζ Puppis standard model star, the rotation velocity where r_t drops from infinity to some finite value is $V_{\rm eq} \approx 410\,{\rm km\ s^{-1}}$. This value is apparently

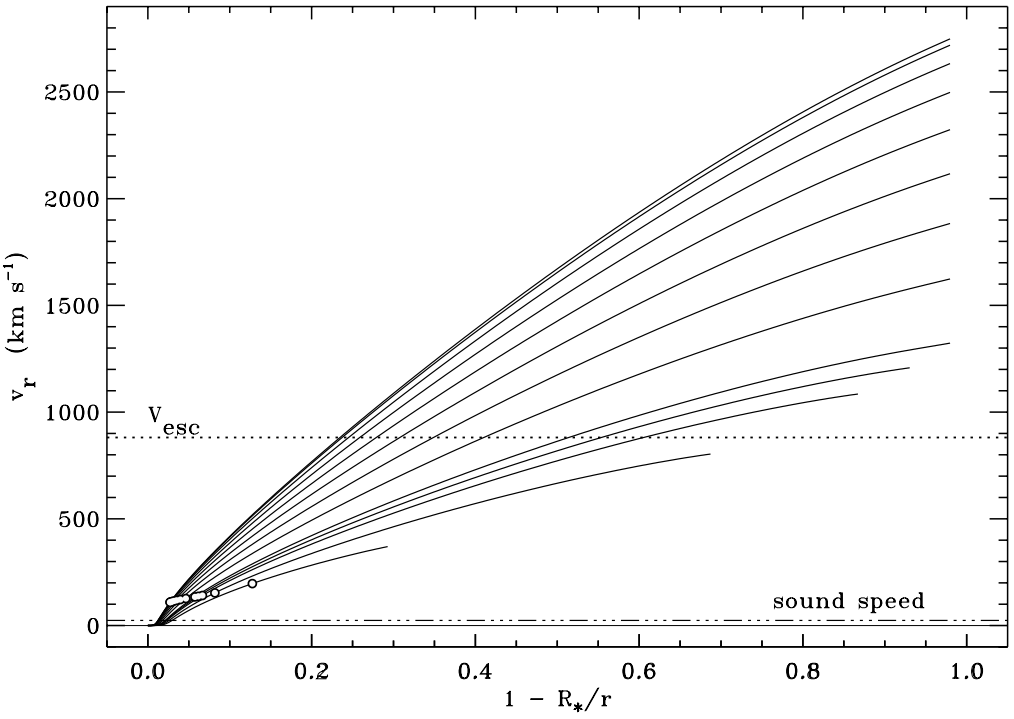

Figure 4.2: Equatorial velocity laws for rotating mCAK models of ζ Puppis. Oblateness and gravity darkening are neglected in these models. From top to bottom, the equatorial rotation velocities are 0, 50, 100, 150, 200, 250, 300, 350, 400, 412.5, 425, 450, 475 km/s. The mCAK critical points for each model are marked by white circles, and the surface escape velocity and sound speed are marked by dashed and dot-dashed lines, respectively. Note the cessation of mCAK wind solutions at *finite radii* for rotation velocities greater than $\sim$410 km/s.

set by the drop in v_∞ to a value just slightly greater than $V_{\rm esc}$, and indeed, for B-stars, where $v_\infty/V_{\rm esc}$ is lower, the rotation speed where r_t becomes finite is also significantly lower. For the ζ Puppis model, the rotation velocity where r_t drops to equal r_c is $V_{\rm eq} \approx 480\,{\rm km\ s^{-1}}$. Numerical VH-1 models for rotation speeds between 410 and 480 km s^{-1} exhibit a well-behaved, time-steady wind for $r < r_t$, and a discontinuity or "kink" in the radial velocity gradient at $r = r_t$. Above this point, no *accelerating* mCAK solutions are available, but a *decelerating* solution is allowed which is extremely close to the pure gravitational "coasting" which would occur if the Sobolev line force were shut off completely. As the rotation velocity of the star increases, the kink-point r_t moves inward, and at some critical value of $V_{\rm eq}$ (still less than $480\,{\rm km\ s^{-1}}$) the decelerating post-kink wind will drop to zero velocity at some $r > r_t$, and the wind will become truly time-dependent. The stalled wind material may fall back down onto the star, and the system would oscillate quasi-stochastically as this limit is reached again and again.

4.2.2 Mass Loss Modulation due to Gravity Darkening

Surprisingly, no models of winds from rotating hot stars have incorporated the effects of gravity darkening. In *radiatively-driven* winds, the surface redistribution of the radiative flux should strongly affect the dynamics of the wind. Cranmer & Owocki (1995, see also Chapter 5) have computed the full vector Sobolev forces from an oblate and gravity-darkened star, but here we use the accuracy of hindsight to examine these effects from a more heuristic, but still reasonably accurate standpoint. As in Section 4.3 below, we present this simplified analysis *before* the full numerical results of Chapter 5 to better familiarize the reader with the various effects in isolation, before seeing them convolved together in the more self-consistent model.

Because of gravity darkening, the continuum radiative flux over the equator decreases as rotation increases, and this has the possibility of reducing the mass loss due to radiative driving, and counteracting the above centrifugal mass loss enhancement. Equations (2.110) and (2.118) can be expressed as a local mass flux per unit area at the stellar surface ($r = R_*$),

$$\dot{m} \equiv \rho v_r = \left\{ \frac{\alpha k^{1/\alpha}}{(1+\alpha) v_{th} c} \left[\frac{(1-\alpha)\sigma_e}{(1+\alpha)c} \right]^{(1-\alpha)/\alpha} \right\} \mathcal{F}^{1/\alpha}\, g_{\rm eff}^{(\alpha-1)/\alpha} \ , \qquad (4.30)$$

and this can be easily extended to the rotating case, where $\mathcal{F}$ and $g_{\rm eff}$ vary with colatitude θ and rotation rate ω. Note that, in general, the line-driving constants α and k vary with temperature (and thus latitude), but for simplicity we assume here they remain fixed. In Section 4.2.1, only the reduction of $g_{\rm eff}$ was taken into account, and it is clear for $\alpha < 1$ that this enhances $\dot{m}$. However, if we assume that the wind "sees" only the *locally* gravity-darkened flux $\mathcal{F}$ at the radius and colatitude

where the local mass loss is determined ($r_c \approx R_*$), we can use the von Zeipel result $\mathcal{F} \propto g_{\rm eff}$ (for $b = 0.25$) to find that

$$\dot{m}(\theta) \propto \mathcal{F}(\theta) \propto g_{\rm eff}(\theta) \ , \tag{4.31}$$

and the pole-to-equator variation of mass flux is independent of α. This implies a *decrease* in mass flux at the equator, where $g_{\rm eff}$ decreases, and an *increase* in mass flux over the poles due to the brighter flux there, compared to a nonrotating star.

For stars exhibiting gravity darkening with an arbitrary von Zeipel exponent b, the variation of mass flux from pole to equator may be increasing *or* decreasing. This can be seen by expressing the local mass flux as

$$\dot{m} \propto \left(K_{vz} g_{\rm eff}^{4b}\right)^{1/\alpha} g_{\rm eff}^{(\alpha-1)/\alpha} \propto g_{\rm eff}^{4(b-b_{crit})/\alpha} \ , \tag{4.32}$$

where $b_{crit} \equiv (1-\alpha)/4$. For $b < b_{crit}$, the mass loss *increases* from pole to equator, as in the non-gravity-darkened case of Section 4.2.1, or $b = 0$. For $b > b_{crit}$, the mass loss *decreases* from pole to equator, as in the fully-radiative case, $b = 0.25$, presented above. For $b = b_{crit}$, (which is equal to 0.1 for $\alpha = 0.6$) the mass flux does not vary with latitude. However, for the early-type O and B stars under consideration here, we expect that $b > b_{crit}$, and that the aforementioned decrease in $\dot{m}$ from pole to equator exists for these stars.

These results are qualitatively different from most other models of winds from rotating stars, which usually predict an equatorial mass loss and density enhancement. Here we find that the bright poles of a rotating hot star eject the densest "plumes" of the wind, and that the equator is both dark and not as dense. Note, however, that the *total* mass loss rate of a rotating star should increase as it spins faster, because, for $b = 0.25$,

$$\dot{M} = \oint \dot{m}\, r^2\, d\Omega \propto K_{vz}^{(1-\alpha)/\alpha} \oint \mathcal{F}\, r^2\, d\Omega \propto K_{vz}^{(1-\alpha)/\alpha} L_* \ , \tag{4.33}$$

and if we assume the bolometric luminosity remains unchanged with rotation, the increase in K_{vz}, or decrease in Σ_1 with increasing ω (see eq. [4.24]) dominates the star-integrated mass loss rate.

Figure 4.3 shows the variation of the mass flux $\dot{m}$ (normalized to the mass flux from a spherical nonrotating star) with colatitude θ and rotation rate ω, for both the pure centrifugal enhancement case of Section 4.2.1 and the von Zeipel ($b = 0.25$) case presented here. In Chapter 5 we compute more rigorously the flux that the wind sees exterior to an oblate and gravity-darkened (uniformly rotating) star, but the approximate results derived above seem to remain qualitatively valid. Thus, in cases where von Zeipel gravity darkening is present, the aforementioned loss of steady-state solutions (the "Koninx effect") should not occur, and the terminal velocity of

the wind may even *increase* over the equator of a rotating star. Of course, if v_∞ remains proportional to $V_{\rm esc}$ (and thus to $g_{\rm eff}$), the trend for the terminal velocity to decrease from pole to equator, and with increasing rotation rate, should remain unchanged.

4.3 Nonradial Radiative Shear Forces

When a radial wind outflow also rotates in the azimuthal direction, the Sobolev line resonances no longer depend only on the *radial* velocity gradient. As derived in Section 2.2.1, the radiative acceleration depends on the projected gradient of the projected velocity component along a given line of sight $\hat{\mathbf{n}}$, which is given by $\hat{\mathbf{n}} \cdot \nabla(\hat{\mathbf{n}} \cdot \mathbf{v})$, and radially asymmetric terms due to rotation can both (1) alter the radial (i.e., mCAK) component of the force, and (2) induce nonradial components of this force. Grinin (1978) first derived the form of these nonradial forces for generalized wind and accretion flows, and MacGregor & Friend (1984) applied them to hot-star winds with magnetic fields. The results of these analyses implied that a non-zero *azimuthal* force can arise in a rotating line-driven wind, but it was not clear if the magnitude of this force would ever be strong enough to significantly affect the radial flow, or in what sense (with or against the direction of rotation) it would act.

Cranmer & Owocki (1995, see also Chapter 5) rederived these general vector radiative forces from a rotating, oblate, and gravity-darkened hot star, but only recently have the dynamical implications of nonradial forces on rotating winds been examined (Owocki, Gayley, & Cranmer 1996). In the spirit of the von Zeipel gravity darkening analysis in the previous Section, here we isolate the azimuthal contribution of the Sobolev nonradial force in the equatorial plane, without considering any other effects of rotation (e.g., oblateness or gravity darkening). Thus, here we outline a simplified theory of radiative driving in a *plane-parallel* (i.e., near-star) environment, and assess the importance of the azimuthal line force which can arise when horizontal "shearing" velocities are present. The original idea for this analysis, and several of the key results herein, are due to K. G. Gayley, and a journal paper on this analysis is currently in preparation.

4.3.1 Plane-Parallel Hydrodynamic Equations

Our goal is to derive analytic relations governing the relative importance of radial and lateral line-driving forces in stellar winds. Because we are concerned mainly with the initial acceleration region of the wind, and thus with radii not too far from the photosphere, we will ignore the *sphericity* of the system, and work in a locally Cartesian frame of reference. (The justification for this approximation

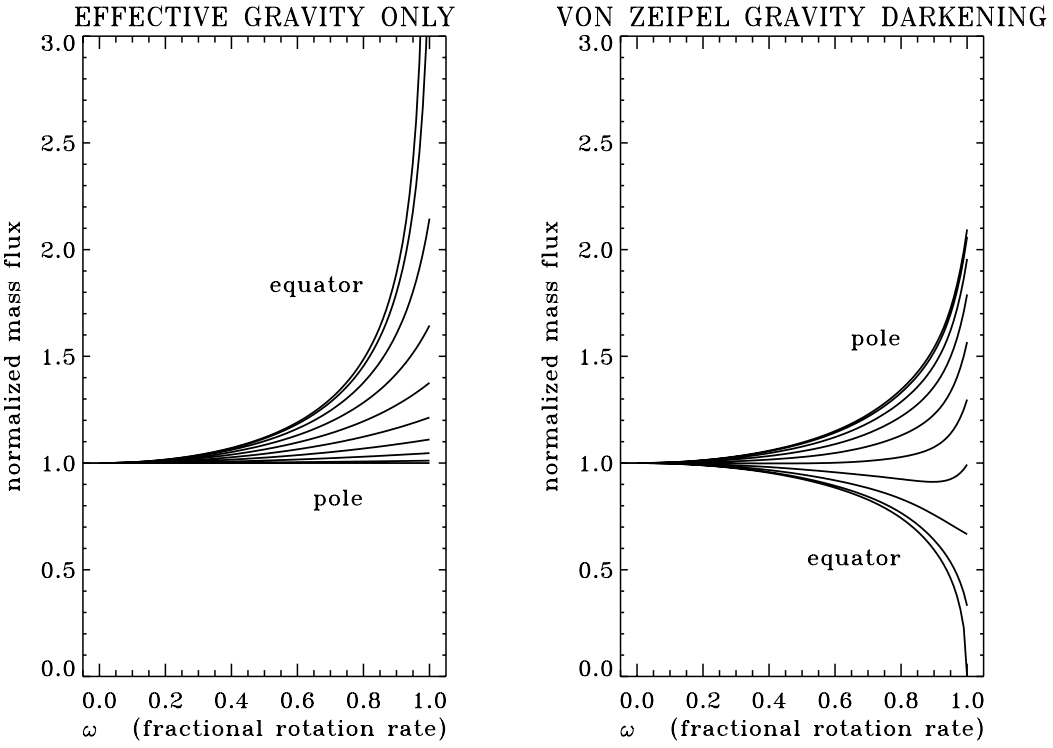

Figure 4.3: Relative mass flux variation with colatitude θ and rotational angular velocity ω, for the pure centrifugal enhancement of Section 4.2.1 (left curves), and the von Zeipel gravity darkening modulation of Section 4.2.2 (right curves). Colatitudes from pole (0 degrees) to equator (90 degrees) are plotted at 10 degree intervals.

will become evident when we determine the radii over which nonradial forces are important.) We define the vertical coordinate z as analogous to radius r, or height $(r - R_*)$, and we define the horizontal coordinate x as analogous to the azimuthal displacement $(r\phi \sin\theta)$, and take specifically $\theta = \pi/2$, or motion in the equatorial plane.

Defining the x and z velocities as u and w, respectively, the equation of mass continuity can be written

$$\frac{\partial \rho}{\partial t} + \frac{\partial}{\partial x}(\rho u) + \frac{\partial}{\partial z}(\rho w) \; = \; 0 \;\; , \tag{4.34}$$

which reduces to the particularly simple form

$$\rho \frac{\partial w}{\partial z} + w \frac{\partial \rho}{\partial z} \; = \; 0 \;\; , \tag{4.35}$$

when we assume time-steady and laterally-symmetric solutions. The assumption of lateral symmetry is equivalent to that of azimuthal symmetry in a rotating spherical system. The mass continuity equation can be integrated to find

$$\rho w \; = \; \dot{m}_0 \;\; , \tag{4.36}$$

which is a planar mass flux in the z direction. This is related to the more common spherical "mass loss rate," $\dot{M} = 4\pi r^2 \dot{m}_0$.

The x and z components of the equation of momentum conservation are

$$\rho \frac{\partial u}{\partial t} + \rho u \frac{\partial u}{\partial x} + \rho w \frac{\partial u}{\partial z} \;\; = \;\; -\frac{\partial P}{\partial x} + \rho g_x^{rad} \tag{4.37}$$

$$\rho \frac{\partial w}{\partial t} + \rho u \frac{\partial w}{\partial x} + \rho w \frac{\partial w}{\partial z} \;\; = \;\; -\frac{\partial P}{\partial z} - \rho g + \rho g_z^{rad} \;\; , \tag{4.38}$$

where g, g_x^{rad}, and g_z^{rad} represent the gravitational and radiative acceleration terms in the x and z directions, respectively. Assuming the above conditions of time-independence and lateral symmetry, together with an isothermal equation of state $(P = \rho a^2)$, these equations simplify to

$$w \frac{\partial u}{\partial z} \;\; = \;\; g_x^{rad} \tag{4.39}$$

$$\left(w - \frac{a^2}{w} \right) \frac{\partial w}{\partial z} \;\; = \;\; g_z^{rad} - g \;\; , \tag{4.40}$$

where eq. (4.35) has been used to eliminate the density gradient in favor of the velocity gradient. The radiative acceleration terms are written in terms of integrals

over the stellar "disk," which in this planar (near-star) limit expands to fill an entire hemisphere. Following the geometrical notation of Cranmer & Owocki (1995),

$$g_z^{rad} = C|w|^\alpha \frac{2}{\pi} \int_{\phi'=0}^{\pi/2} \int_{\mu'=0}^{1} \left(\left| \frac{\partial v_\ell}{\partial \ell} \right|_+^\alpha + \left| \frac{\partial v_\ell}{\partial \ell} \right|_-^\alpha \right) \mu' \, d\mu' \, d\phi' \tag{4.41}$$

$$g_x^{rad} = C|w|^\alpha \frac{2}{\pi} \int_{\phi'=0}^{\pi/2} \int_{\mu'=0}^{1} \left(\left| \frac{\partial v_\ell}{\partial \ell} \right|_+^\alpha - \left| \frac{\partial v_\ell}{\partial \ell} \right|_-^\alpha \right) \sqrt{1-\mu'^2} \, d\mu' \, \sin\phi' \, d\phi' \,, \tag{4.42}$$

with the constant C defined in the plane-parallel limit as

$$C \equiv \frac{GM_*, \; k}{R_*^2} \left(\frac{1}{\dot{m}_0 \, \sigma_e v_{th}} \right)^\alpha \tag{4.43}$$

and the line-of-sight velocity gradient, $\hat{\mathbf{n}} \cdot \nabla (\hat{\mathbf{n}} \cdot \mathbf{v})$, is written here as

$$\left(\frac{\partial v_\ell}{\partial \ell} \right)_\pm = \mu'^2 \left(\frac{\partial w}{\partial z} \right) \pm \mu' \sqrt{1-\mu'^2} \, \sin\phi' \left(\frac{\partial u}{\partial z} \right) \quad . \tag{4.44}$$

4.3.2 Zero-Order Solutions

First, consider solutions to the equations of motion without any radiative acceleration terms. For a nontrivial wind solution ($w \neq 0$), eq. (4.39) implies that the horizontal velocity u must be constant in z. The z-momentum equation, eq. (4.40), similarly implies the implicit Parker-like solution for $w(z)$:

$$a^2 \ln \left(\frac{w}{w_0} \right) - \frac{1}{2} \left(w^2 - w_0^2 \right) = gz \quad , \tag{4.45}$$

with the assumptions that g is constant in the near-star region of interest, and that $w(z=0) \equiv w_0$. In the supersonic ($w \gg a$) limit, the sound-speed-dependent term in the equation of motion can be neglected, and

$$w(z) \approx \sqrt{w_0^2 - 2gz} \quad . \tag{4.46}$$

In the extremely subsonic ($w \ll a$) limit, the inertial term in the equation of motion, proportional to $w(\partial w / \partial z)$, can be neglected, and

$$w(z) \approx w_0 \exp(z/H) \quad , \tag{4.47}$$

where the isothermal scale height $H \equiv a^2/g$.

The standard analysis of radiatively-driven stellar winds usually assumes that the horizontal radiative force g_x^{rad} is negligible when compared to the radial radiative

force g_z^{rad}. In our plane-parallel approximation, this is equivalent to assuming that $\partial u/\partial z = 0$. Note that the horizontal velocity itself (u) does not appear in any of the equations of motion, so it can be set to an arbitrary constant. Although we will eventually be concerned with "steep" shearing solutions (i.e., *large* values of $|\partial u/\partial z|$), the behavior of solutions in the limit of small horizontal gradients will be instructive to decide whether large solutions are even *possible* (see Figure 4.4).

The radial radiative force, in the limit of a vanishing horizontal velocity gradient, can be reduced to the particularly simple form:

$$g_z^{rad} = C \left| w \frac{\partial w}{\partial z} \right|^{\alpha} \frac{2}{\pi} \int_{\phi'=0}^{\pi/2} \int_{\mu'=0}^{1} |2\mu'|^{\alpha} \, \mu' \, d\mu' \, d\phi' \tag{4.48}$$

$$= C \left| w \frac{\partial w}{\partial z} \right|^{\alpha} \left(\frac{1}{1+\alpha} \right) \quad . \tag{4.49}$$

Using this, one can write the CAK equation of motion (eq. [4.40]) as

$$F_1 \equiv \left(1 - \frac{a^2}{w^2} \right) y + g - \frac{C}{1+\alpha} |y|^{\alpha} = 0 \quad , \tag{4.50}$$

with $y \equiv w(\partial w/\partial z)$. Since the CAK critical point is often seen to occur in the supersonic portion of the wind, we can analyze this equation in the limit of *zero-sound-speed,* and write the singularity condition,

$$\frac{\partial F_1}{\partial y} = 1 - \frac{\alpha C}{1+\alpha} |y|^{\alpha - 1} = 0 \quad , \tag{4.51}$$

and these two equations can be solved uniquely for C, which is related to the mass loss rate, and y_c, the critical value of the radial velocity gradient. Thus,

$$y_c = g \left(\frac{\alpha}{1-\alpha} \right) \quad , \qquad C |y_c|^{\alpha} = g \left(\frac{1+\alpha}{1-\alpha} \right) \quad . \tag{4.52}$$

In the region of z-values of interest, $y = y_c$ is *constant,* and the definition of y can be integrated to find

$$w(z) \approx \sqrt{w_0^2 + 2 \left(\frac{\alpha}{1-\alpha} \right) g z} \quad , \tag{4.53}$$

which is very similar to the above eq. (4.46), with the radiative acceleration counteracting gravity. Thus, in the spirit of the approximations in eqs. (4.46) and (4.47), we can *fit* the entire run of $w(z)$ from subsonic to supersonic velocities by the implicit solution of

$$a^2 \ln \left(\frac{w}{a} \right) + \frac{1-\alpha}{2\alpha} \left(w^2 - a^2 \right) = g z \quad , \tag{4.54}$$

where we have set $w_0 = a$.

4.3.3 Taylor Series Shear Analysis

The horizontal radiative acceleration is identically zero in the limit $\partial u/\partial z = 0$, but it will be instructive to determine the quantity $\partial g_x^{rad}/\partial(\partial u/\partial z)$, which is the *slope* of this force, in the limit of small horizontal velocity gradients. Figure 4.4 shows a relatively strong and weak horizontal radiative acceleration, plotted along with the inertial term (the left side of eq. [4.39]), both versus $\partial u/\partial z$. When the slope of g_x^{rad} – in the vicinity of the origin – is smaller than that of the straight line, the only solution available is the trivial one, $\partial u/\partial z = 0$. However, when the slope of g_x^{rad} is larger than that of the straight line, other "steep" shearing solutions become available. It is our goal to determine when these solutions are allowed in a line-driven wind.

The horizontal equation of momentum conservation can be written in terms of a new variable $\Psi \equiv (\partial u/\partial z)/(\partial w/\partial z)$, as

$$\Psi \;=\; C|y|^{\alpha-1}\,\frac{2}{\pi}\int_{\phi'=0}^{\pi/2}\int_{\mu'=0}^{1}\left(F_+ - F_-\right)\,\sqrt{1-\mu'^2}\;d\mu'\,\sin\phi'\,d\phi' \quad , \tag{4.55}$$

where here the line-of-sight velocity gradient terms have been scaled to

$$F_\pm \;\equiv\; \left|\mu'^2 \pm \Psi\,\mu'\sqrt{1-\mu'^2}\,\sin\phi'\right|^{\alpha} \quad . \tag{4.56}$$

Expanding to first order about $\Psi = 0$,

$$F_\pm(\Psi) \;=\; F_\pm(0) \;+\; \Psi\left(\frac{\partial F_\pm}{\partial \Psi}\right)_{\Psi=0} \;+\; \cdots \tag{4.57}$$

$$\approx\; \mu'^{2\alpha} \;\pm\; \alpha\Psi\mu'^{2\alpha-1}\sqrt{1-\mu'^2}\,\sin\phi' \quad . \tag{4.58}$$

The horizontal momentum conservation equation becomes, upon substituting $y = y_c$ from above,

$$\Psi \;=\; C|y_c|^{\alpha-1}\,\frac{4\alpha\Psi}{\pi}\int_{\phi'=0}^{\pi/2}\sin^2\phi'\,d\phi'\int_{\mu'=0}^{1}\left(\mu'^{2\alpha-1}-\mu'^{2\alpha+1}\right)\,d\mu' \tag{4.59}$$

$$=\; \left(\frac{1+\alpha}{\alpha}\right)\left(\frac{\Psi}{2(1+\alpha)}\right) \;=\; \frac{\Psi}{2\alpha} \quad , \tag{4.60}$$

which implies that, to obtain steep solutions in Figure 4.4, we require $\alpha < (1/2)$. This is a stringent limit which applies in the *supersonic* wind, and for realistic values of α, no shear solutions should be possible in the majority of the wind.

Note that the above analysis assumed a radial velocity gradient $y = y_c$ as given by the supersonic critical point analysis. In the *subsonic* region of the wind,

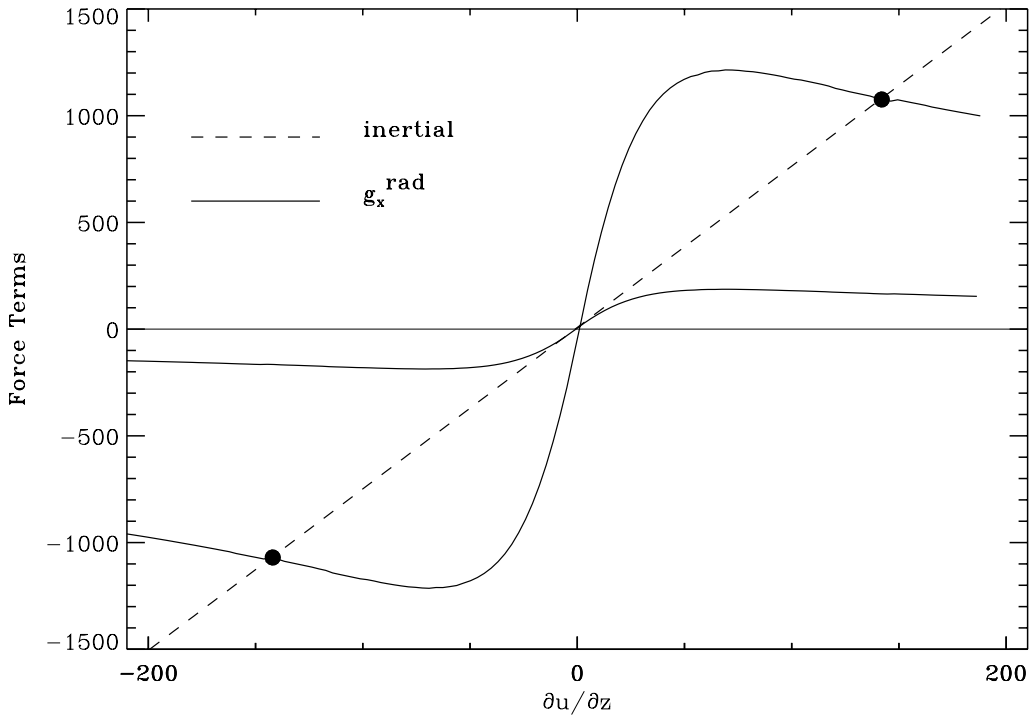

Figure 4.4: Horizontal radiative acceleration (solid lines) and inertial acceleration $w\,\partial u/\partial z$ (dashed line), plotted as a function of the vertical gradient of the horizontal velocity. A weak horizontal acceleration only satisfies the equations of motion for $\partial u/\partial z = 0$, but a strong horizontal acceleration also has "steep" shear solutions (filled circles) for large values of $|\partial u/\partial z|$.

this does not apply, and we can assume the radial velocity law given by eq. (4.47), implying that

$$y = \frac{w^2}{H} = \frac{w_0^2}{H}\exp(2z/H) \quad . \tag{4.61}$$

However, let us still assume that the mass-loss constant C is still given by the supersonic critical point analysis, since the mass flux is thought to be determined at that point. If we define $w_0 = a$, then, for negative z-values,

$$\Psi = C|y_c|^{\alpha-1}\left|\frac{y}{y_c}\right|^{\alpha-1}\left(\frac{\Psi}{2(1+\alpha)}\right) \tag{4.62}$$

$$= \Psi\left(\frac{\alpha}{1-\alpha}\right)^{1-\alpha}\frac{1}{2\alpha}\exp\left[-\frac{2z}{H}(1-\alpha)\right] \tag{4.63}$$

$$= \frac{\Psi}{2\alpha}\left[\left(\frac{\alpha}{1-\alpha}\right)^{1-\alpha}\left(\frac{w}{a}\right)^{2\alpha-2}\right] \equiv \frac{\Psi}{2\alpha}\zeta(\alpha,w) \quad . \tag{4.64}$$

For example, if $\alpha = 0.5$, the condition for steep solutions is simply $w < a$, but if $\alpha = 0.7$, the condition reduces to $w \lesssim 0.872\,a$. Clearly if $w \approx a$ the subsonic approximation breaks down, but these results conclusively show that extremely subsonic winds have a steep shear solution available for $\partial u/\partial z$. Unfortunately the magnitudes of *all* radiative forces are small in the deeply subsonic wind, and it is not clear how important these solutions will be at this depth.

4.3.4 Higher Order Shear Estimates

The above first-order Taylor series analysis tells us only if steep shearing solutions are or are not present. By going to higher order, we can model the "concavity" of $g_x^{rad}(\Psi)$ sufficiently well to actually solve for the steep value of Ψ. To simplify matters somewhat, note that the z-component of the radiative acceleration, $g_z^{rad}(\Psi)$ is an *even* function in powers of Ψ, and the x-component is an *odd* function in powers of Ψ. Thus, the scaled line-of-sight velocity gradient $F_\pm$ (eq. [4.56]) needs to be expanded at least to *third* order, to take into account the next highest order terms in both g_x^{rad} and g_z^{rad}:

$$F_\pm(\Psi) = F_\pm(0) + \Psi\left(\frac{\partial F_\pm}{\partial\Psi}\right)_0 + \frac{1}{2}\Psi^2\left(\frac{\partial^2 F_\pm}{\partial\Psi^2}\right)_0 + \frac{1}{6}\Psi^3\left(\frac{\partial^3 F_\pm}{\partial\Psi^3}\right)_0 + \cdots \tag{4.65}$$

$$\approx \mu'^{2\alpha} \pm \alpha\Psi\mu'^{2\alpha-1}\sqrt{1-\mu'^2}\,\sin\phi' \tag{4.66}$$

$$+ \frac{1}{2}\alpha(\alpha-1)\Psi^2\mu'^{2\alpha-2}(1-\mu'^2)\,\sin^2\phi' \tag{4.67}$$

$$\pm \frac{1}{6}\alpha(\alpha-1)(\alpha-2)\Psi^3\mu'^{2\alpha-3}(1-\mu'^2)^{3/2}\,\sin^3\phi' \quad . \tag{4.68}$$

Performing the angle integrations yields, for both components of the radiative acceleration,

$$g_z^{rad} \approx \frac{C}{1+\alpha}|y|^{\alpha}\left[1-\frac{1}{4}\Psi^2(1-\alpha)\right] \tag{4.69}$$

$$g_x^{rad} \approx \frac{C}{1+\alpha}|y|^{\alpha}\left(\frac{\Psi}{2}\right)\left[1-\frac{1}{4}\Psi^2(2-\alpha)\right] \quad . \tag{4.70}$$

Note that the critical-point solution to the vertical momentum conservation equation implies

$$C|y_c|^{\alpha-1} = \left(\frac{1+\alpha}{\alpha}\right)\frac{1}{1-\Psi^2(1-\alpha)/4} \quad , \tag{4.71}$$

with y_c defined as before, and the horizontal momentum conservation equation becomes (compare to eq. [4.62])

$$\Psi = \frac{\Psi}{2\alpha}\left[\frac{1-\Psi^2(2-\alpha)/4}{1-\Psi^2(1-\alpha)/4}\right]\left|\frac{y}{y_c}\right|^{\alpha-1} \tag{4.72}$$

$$= \frac{\Psi}{2\alpha}\left[\frac{1-\Psi^2(2-\alpha)/4}{1-\Psi^2(1-\alpha)/4}\right]\zeta(\alpha,w) \quad , \tag{4.73}$$

generalizing the notation defined for the *subsonic* wind in eq. (4.64). This last equation can be solved for the steep (nontrivial) solution,

$$\Psi = \sqrt{\frac{4(\zeta-2\alpha)}{2\alpha^2-(2+\zeta)\alpha+2\zeta}} \quad , \tag{4.74}$$

where $\zeta = 1$ if we assume $y = y_c$ in the supersonic wind. Figure 4.5 shows solutions for $w(z)$, from eq. (4.54), and $(\partial u/\partial z)$, as given above, for the specified $(\partial w/\partial z)$ and various values of α. Note that there is a relatively small and *finite* range of z-values for which there exists a significant horizontal shear for realistic ($\alpha > 0.5$) CAK winds, and the plane-parallel approximation in this Section is reasonably justified.

4.3.5 Stability of Shear Flows

The steep shear solutions derived above, which emerge from the photosphere with appreciable vertical gradients in both the u and w velocities, may or may not be stable to small perturbations. Let us review the conditions necessary for horizontal velocities to cause a convective instability in a plane-parallel atmosphere (see, e.g., Moss & Smith 1981). Consider a static and stratified medium which is convectively *stable,* i.e., with a Brunt-Väisälä oscillation frequency,

$$\omega_{BV}^2 = \frac{g}{\rho}\left[\left(\frac{\partial\rho}{\partial z}\right)_{ad} - \left(\frac{\partial\rho}{\partial z}\right)\right] \tag{4.75}$$

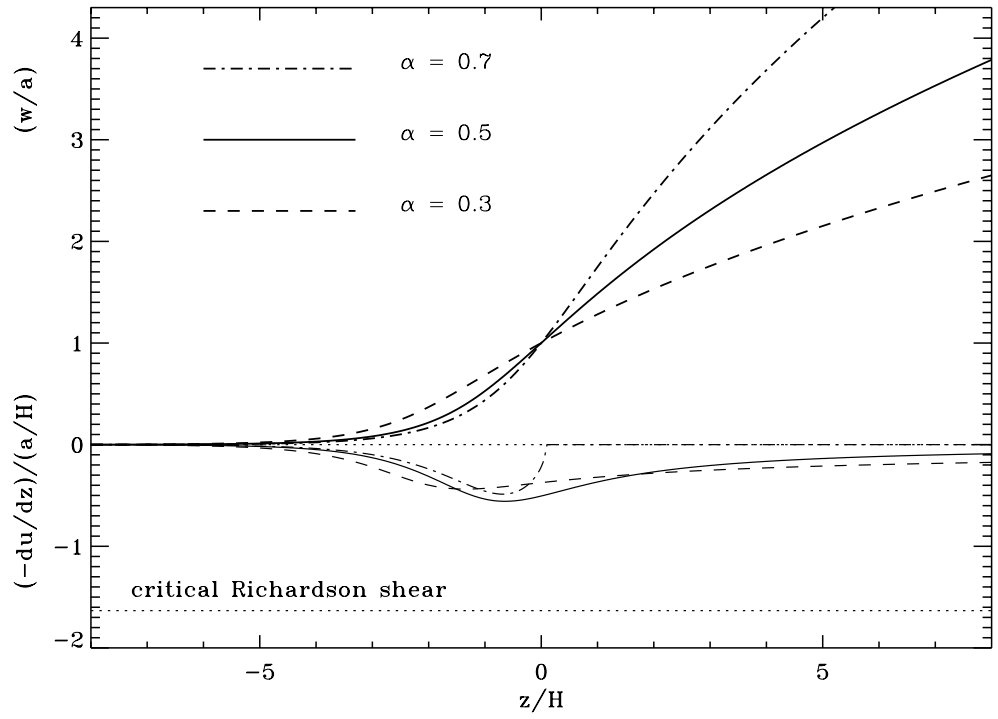

Figure 4.5: Upper curves: vertical velocity laws $w(z)$ for different mCAK α exponents, plotted versus height z, which is taken to be zero at the sonic point. **Lower curves:** dimensionless "steep" shear solutions from the third-order Taylor expansion of Ψ. The integrated "buildup" in u can be estimated by inspection to be limited only to a few sound speeds.

$$= \frac{g^2}{a^2}(\gamma - 1) > 0 \ , \tag{4.76}$$

where here the sound speed a is the *adiabatic* sound speed $(\gamma P/\rho)^{1/2}$, and eq. (4.76) is the Brunt-Väisälä frequency for an *isothermal* stratified atmosphere (see Chapter 7). The average force per unit volume felt by an oscillating parcel of gas, during a complete cycle of displacement, is approximately equal to

$$\Delta f \approx \frac{1}{2}\omega_{BV}^2 \rho \Delta z \ , \tag{4.77}$$

where the blob moves a mean distance Δz in one half-period of motion. The work (per unit mass) required to *interchange* two similar blobs, initially at heights z and $z + \Delta z$, is given by

$$\Delta W \approx \frac{2\Delta f}{\rho}\Delta z \approx \omega_{BV}^2 (\Delta z)^2 \ . \tag{4.78}$$

If we consider the possibility that *shear forces* can provide the work necessary to overturn these otherwise convectively *stable* parcels, we can express this work in terms of the kinetic energy stored in the relative horizontal motion of different layers. Assuming our two "stacked" blobs have horizontal speeds u and $u + \Delta u$, and also assuming that their *mixing* eventually yields a mean speed $u + \Delta u/2$, the difference in kinetic energies (per unit mass) between the initial and final states is

$$\Delta K = \frac{1}{2}u^2 + \frac{1}{2}(u + \Delta u)^2 - \frac{1}{2}\left[2\left(u + \frac{1}{2}\Delta u\right)^2\right] \tag{4.79}$$

$$= \frac{1}{4}(\Delta u)^2 \ , \tag{4.80}$$

indicating that the addition of shear in *any* horizontal direction produces extra positive kinetic energy which can drive a Kelvin-Helmholz instability. However, in our stratified medium, we only have instability if this kinetic energy outweighs the work needed to disrupt the convective stability, or

$$\Delta K > \Delta W \ . \tag{4.81}$$

This condition can be written in terms of the dimensionless *Richardson number,*

$$\mathrm{Ri} \equiv \frac{\Delta W}{4\,\Delta K} = \frac{\omega_{BV}^2 (\Delta z)^2}{(\Delta u)^2} \approx \frac{\omega_{BV}^2}{(\partial u/\partial z)^2} \ , \tag{4.82}$$

and the medium is stable when $\mathrm{Ri} \gtrsim (1/4)$ and unstable when $\mathrm{Ri} \lesssim (1/4)$. For an isothermal atmosphere, we can derive a critical value of the vertical gradient of the horizontal velocity, using $\mathrm{Ri} = 1/4$, and

$$\left(\frac{\partial u}{\partial z}\right)_{\mathrm{crit}} = \frac{2g}{a}\sqrt{\gamma - 1} \approx 1.63\left(\frac{a}{H}\right) \ , \tag{4.83}$$

for $\gamma = 5/3$. Note from Figure 4.5 that the magnitude of the "steep" shear solutions of $\partial u/\partial z$ are well *below* this critical value, implying their stability to shear-induced convective mixing.

The present plane-parallel analysis does not distinguish between steep *spin-up* azimuthal velocities ($\partial u/\partial z > 0$) and steep *spin-down* azimuthal velocities ($\partial u/\partial z < 0$). This degeneracy is lifted in the fully three-dimensional models in spherical coordinates presented in Chapter 5. A test point in the wind over a spherical star sees a distinct difference between the approaching and receding limbs of the rotating stellar disk, and the different Doppler shifts of stellar photons cause a definite bias toward azimuthal forces in the *opposite* direction to the rotation. Spin-down solutions are almost always favored in winds which rotate slower than the rigid body of the star, and this rapid decrease in $v_\phi(r)$ is able to rob the wind of a fraction of its angular momentum.